Proceedings of the 37th IEEE
Conference on Decision & Control
Tampa, Florida USA • December 1998

Complex Dynamics in Repeated Impact Oscillators [1]

S. Salapaka*, M.V. Salapaka+, M. Dahleh* and I. Mezić*

*Department of Mechanical and Environmental Engineering, University of California, Santa Barbara, CA 93106, U.S.A.

salpax@engineering.ucsb.edu, dahleh@engineering.ucsb.edu,mezic@engineering.ucsb.edu

+Electrical Engineering Department, Ames, Iowa IA 50011, U.S.A.

murti@iastate.edu

Abstract

This work deals with a model for repeated impacts of a mass attached to a spring with a massive, sinusoidally vibrating table. This model has been studied in an attempt to understand the cantilever-sample dynamics in atomic force microscopy. In this work, we have shown that for some values of the frequency of the vibrating table, there are countably many orbits of arbitrarily long periods and the system is sensitive to the initial conditions with which the experiments are conducted.

1 Introduction

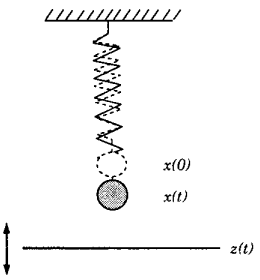

Figure 1: The model for cantilever-sample system.

In this paper, we consider a spring-mass system with natural frequency ω_n, and a massive table vibrating below it such that the rest positions of the table and the mass are not the same (the case when they are the same is studied in [1]). Figure(1) shows the visualization of the system. Here all variables are measured from the equilibrium position of the mass and the upward direction is considered as positive. The rest position of the mass is at $x = 0$ and the position of the table is described by the equation $z(t) = -p + \beta\sin(\omega t)$. It is assumed that the mass of the table is large and therefore its motion is not altered by the impacts between the mass and the table. The equation governing the motion of the mass under no external forcing is given by

$$\ddot{x} + {\omega_n}^2 x = 0. \quad (1)$$

[1]This research was partly supported by NSF ECS-9632820, AFOSR F49620-97-1-0168 and NSF ECS-9733802.

The solution to this differential equation with initial displacement x_o and initial velocity $\dot{x}_o$ (at $t = t_0$) is given by

$$x(t) = x_o\cos(\omega_n(t-t_0)) + \frac{\dot{x}_o}{w_n}\sin(\omega_n(t-t_0)), \quad (2)$$

$$\dot{x}(t) = \dot{x}_o\cos(\omega_n(t-t_0)) - \omega_n x_o\sin(\omega_n(t-t_0)). \quad (3)$$

The dissipation of energy by the mass in an impact is captured by the coefficient of restitution ϵ. To study this model, we have to solve the differential equation (1) repeatedly with initial conditions being redefined at every impact. If we denote the sequence of time instants at which the impacts take place by $\{t_k\}, k \in \mathbb{N}$, and the speed of the mass just before the impact at time instant t_k by v_k, then the motion of the mass in the time interval $(t_k, t_{k+1}]$ is given by equations (2) and (3), where the initial conditions are given by the following equations,

$$x_o = -p + \beta\sin(\omega t_k) \quad (4)$$

$$\dot{x}_o = -\epsilon v_k + (1+\epsilon)\beta\omega\cos(\omega t_k). \quad (5)$$

These equations hold for the impacts after which the mass and the table separate (that is, $x(t) - z(t) > 0$ for all $t \in (t_k, t_{k+1})$). We know that at the instant t_{k+1}, the following relations hold,

$$x(t_{k+1}) - z(t_{k+1}) = 0 \quad (6)$$

$$v_{k+1} = \dot{x}(t_{k+1}), \quad (7)$$

where the initial conditions are given by (4) and (5). After substituting (4),(5),(2) and (3) in (6) and (7), we obtain the following equations,

$$(-p + \beta\sin(\omega t_k))\cos(\omega_n(t_{k+1}-t_k)) + \frac{-\epsilon v_k + (1+\epsilon)\beta\omega\cos(\omega t_k)}{\omega_n}\sin(\omega_n(t_{k+1}-t_k)) + p - \beta\sin(\omega t_{k+1}) = 0, \quad (8)$$

$$v_{k+1} = (\omega_n p - \beta\omega_n\sin(\omega t_k))\sin(\omega_n(t_{k+1}-t_k)) + ((\epsilon+1)\beta\omega\cos(\omega t_k) - \epsilon v_k)\cos(\omega_n(t_{k+1}-t_k)). \quad (9)$$

Note that the above equations are transcendental and therefore cannot be solved in a closed form. We also see that, in the case of inelastic impacts (i.e. $\epsilon = 0$), equation (8) becomes independent of the speed v_k. Physically, this corresponds to the impacts in which there is

0-7803-4394-8/98 $10.00 © 1998 IEEE

no rebound. In this case the knowledge of the position of the table at impact completely determines the motion of the mass and therefore we do not need to know the velocity of the mass just before impact. Even though the impacts are inelastic, the mass and the table will eventually separate because of the restoring force of the spring and the vibration of the table. We nondimensionalize equation (8) by introducing the variables; scaled impact time $\psi_k = \omega t_k$, the amplitude $\nu = \frac{-\beta}{p}$ and the frequency ratio $\eta = \frac{\omega_n}{\omega}$. This results in the following equation for the inelastic case (i.e. $\epsilon = 0$),

$$\begin{aligned}(1+\nu\sin(\psi_k))\cos(\eta(\psi_{k+1}-\psi_k)) \qquad (10)\\ +\frac{\nu}{\eta}\cos(\psi_k)\sin(\eta(\psi_{k+1}-\psi_k))\\ -1-\nu\sin(\psi_{k+1})=0.\end{aligned}$$

Related to the scaled impact time, we introduce a phase variable, $\phi := \psi \ modulo\ 2\pi$. This variable gives the position of the table at time instant ϕ. We know that, when the impacts are inelastic, given an impact phase, the next phase at which impact occurs is uniquely determined. We denote this mapping by $f_{\eta,\nu} : \phi_i \to \phi_{i+1}, \phi \in [0, 2\pi)$.

2 Sensitive Dependence on Initial Conditions: Inelastic Impacts

In the following sections it will be shown that the map $f_{\eta,\nu} : \phi_i \to \phi_{i+1}$ is sensitive to initial conditions for certain parameter values. Note that this map cannot be obtained analytically as equation (10) is transcendental. However, this function can be constructed by numerical means for a given value of η and over a discrete set of values of phase, $\phi \in [0, 2\pi]$.

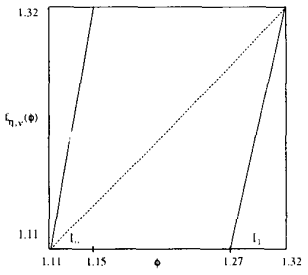

Figure 2: The map $f_{\eta,\nu}$ for $\eta = .2121$ and $\nu = -0.2$. $f_{\eta,\nu}(\phi)$ for ϕ in $[1.15, 1.27]$ is not in $[1.11, 1.32]$ and not shown in this Figure.

In Figure (2), we show the plot $f_{\eta,\nu}$ versus ϕ with $(\eta, \nu) = (0.2121, -0.2)$ and $\phi \in I := [1.11, 1.32]$. Note that the interval has been partitioned into three smaller intervals and I_0 and I_1 are closed intervals. Let Λ be set of all those points in I that are not mapped out of I by repeated application of $f_{\eta,\nu}$ on them. That is,

$$\begin{aligned}\Lambda &= \{\phi \in I : f^n_{\eta,\nu}(\phi) \in I \text{ for all } n \in \mathbb{N}\}\\ &= \bigcap_{n=0}^{\infty} f^{-n}_{\eta,\nu}(I).\end{aligned}$$

Note that, if $\phi \in \Lambda$, then ϕ has to be in $I_0 \cup I_1$, because if $\phi \notin I_0 \cup I_1$ then $f_{\eta,\nu}(\phi) \notin I$ (see Figure 2) . To every point, ϕ_0 in Λ we can associate a sequence $\{\alpha_k\}, k \in \mathbb{N}$ such that

$$\alpha_k = 0 \text{ if } f^k_{\eta,\nu}(\phi_0) \in I_0,$$

$$\alpha_k = 1 \text{ if } f^k_{\eta,\nu}(\phi_0) \in I_1.$$

This is always possible since otherwise $f^{k+1}_{\eta,\nu}(\phi_0) \notin I$. We define a space of infinite sequences, Σ by

$$\Sigma = \{0.x_1x_2.... \text{ such that } x_i \in \{0,1\} \text{ for all } i \in \mathbb{N}\}.$$

We also define a map $h : \Lambda \to \Sigma$ by $h(\phi_0) = 0.\alpha_1\alpha_2\alpha_3...$, where $\alpha_k, k \in \mathbb{N}$ are obtained as described above. We have introduced these sequences into this analysis because it can be shown that the space of these sequences is homeomorphic to the invariant set Λ. Thus we can find the properties of the underlying set Λ by studying Σ. In the next section, we will study this sequence space.

2.1 Symbolic Dynamics

A good reference of this material can be found in [5]. We define a metric $d(\cdot,\cdot)$ on Σ by $d(x,y) = \sum_{i=1}^{\infty} \frac{|x_i - y_i|}{2^i}$, where $x = 0.x_1x_2x_3..., y = 0.y_1y_2y_3...$. Let $s^i, i \in \mathbb{N}$ denote all finite binary sequences of i bits. Note that for every $i \in \mathbb{N}$ there exist 2^i i-bit sequences. Let us denote these by $s^i_1, s^i_2, ...s^i_{2^i}$. We also define, the shift map $\sigma : \Sigma \to \Sigma$ by $\sigma(0.x_1x_2x_3...) = 0.x_2x_3x_4....$
The sequence of binary sequences generated by repeated application of the map σ to a point in Σ is called an *orbit* of σ. An orbit of σ is *i-periodic* (or has *period i*) if $\sigma^i(x) = x$ for all x in the orbit. Now, we state three facts concerning the dynamics of σ on Σ in the following theorem.

Theorem 1 *The shift map σ has*
1. countably many periodic orbits of arbitrarily high periods;
2. uncountably many nonperiodic orbits;
3. a dense orbit.

Proof: See [5] for proof.

From Figure(2), we note that $\gamma_1 := 5.25 \geq \frac{\partial f_{\eta,\nu}}{\partial \phi} \geq \gamma_2 := 4.2$ for all $\phi \in int(I_0) := (c_0, d_0) = (1.11, 1.15)$ and for all $\phi \in int(I_1) := (c_1, d_1) = (1.27, 1.32)$. Also note the function $f_{\eta,\nu}$ is monotonically increasing on I_0 and I_1 and therefore $f^{-1}_{\eta,\nu}(J)$ consists of two closed intervals, one in I_0 and another in I_1, where J is any closed interval in I_0 or I_1. Also, the length of each of these intervals is less than $\frac{1}{\gamma_2}|J|$ where $|J|$ represents the usual length of the interval.

Theorem 2 *The map $h : \Lambda \to \Sigma$ is a homeomorphism.*

Proof: We need only to show that h is one-one, onto and continuous since the continuity of the inverse of h will follow from the fact that one-one, onto and continuous maps from compact sets into Hausdorff spaces are homeomorphisms [5].

Let $I_{\alpha_1\alpha_2\ldots\alpha_n}$ denote the set, $I_{\alpha_1} \cap f^{-1}_{\eta,\nu}(I_{\alpha_2}) \cap f^{-2}_{\eta,\nu}(I_{\alpha_3}) \ldots \cap f^{-n+1}_{\eta,\nu}(I_{\alpha_n}) = I_{\alpha_1} \cap f^{-1}_{\eta,\nu}(I_{\alpha_2} \cap f^{-1}_{\eta,\nu}(I_{\alpha_3} \ldots \cap f^{-1}_{\eta,\nu}(I_{\alpha_n})\ldots))$ where $\alpha_i \in \{0,1\}$. Note that for every point ϕ in $I_{\alpha_1\alpha_2\ldots\alpha_n}$, $h(\phi) = .\beta_1\beta_2\ldots$ is such that $\beta_i = \alpha_i, i \in \{1,2\ldots n\}$. As $f^{-1}_{\eta,\nu}(I_{\alpha_k}) \cap I_j$ is a closed interval for all $k \in \mathbb{N}, j \in \{0,1\}$, $I_{\alpha_1\alpha_2\ldots\alpha_n}$ is a closed interval. From the definition of $I_{\alpha_1\alpha_2\ldots\alpha_n}$, it follows that $I_{\alpha_1\alpha_2\ldots\alpha_{n+1}} \subset I_{\alpha_1\alpha_2\ldots\alpha_n}$. As the slope of $f_{\eta,\nu} > \gamma_2$ at all points in $I_j, j \in \{0,1\}$, $|I_{\alpha_1\alpha_2\ldots\alpha_{n+1}}| < \frac{1}{\gamma_2}|I_{\alpha_1\alpha_2\ldots\alpha_n}|$.

h is one-one: This means that given $\phi, \phi' \in \Lambda$, if $\phi \neq \phi'$, then $h(\phi) \neq h(\phi')$. Let us prove by contradiction, suppose $\phi \neq \phi'$ and

$$h(\phi) = h(\phi') = .x_1x_2\ldots x_n\ldots;$$

then by construction of Λ we know that $\phi \in I_{x_1x_2\ldots x_n}$ and $\phi' \in I_{x_1x_2\ldots x_n}$ for all $n \in \mathbb{N}$. But, $\{I_{x_1x_2\ldots x_n}\}$ is a nested sequence of closed bounded intervals whose lengths shrink to zero, therefore by a theorem due to Cantor (see Theorem 1.2 in [3]), $\cap_{n=1}^{\infty} I_{x_1x_2\ldots x_n}$ contains a unique point, and hence $\phi = \phi'$. However, this contradicts our supposition that $\phi \neq \phi'$. This shows h is *one − one*.

h is onto: Let $y = .y_1y_2\ldots \in \Sigma$ be arbitrarily chosen. By Cantor's theorem, we know that $\cap_{n=1}^{\infty} I_{y_1y_2\ldots y_n}$ is a unique point in Λ. Let this point be denoted by ϕ_1. Then by construction of Λ and definition of h we have that $y = h(\phi_1)$. As y was chosen arbitrarily in Σ, we have shown that h is an *onto* function.

h is continuous: This means that given any point $\psi \in \Lambda$ and $\epsilon > 0$, we can find a $\delta > 0$ such that $|\psi' - \psi| < \delta$ implies $d(h(\psi'), h(\psi)) < \epsilon$. Let $\epsilon > 0$ and $\psi \in \Lambda$ with $h(\psi) = 0.\psi_1\psi_2\ldots$ be given. From the definition of the metric on Σ, we know that there exists $N = N(\epsilon)$ in $\mathbb{N}$ such that for any $z = 0.z_1z_2\ldots \in \Sigma$ with $z_i = \psi_i, i \in \{1,2\ldots N\}$, $d(h(\psi), z) < \epsilon$. We know that for each θ in Λ such that $|\psi - \theta| < \delta := \frac{1}{\gamma_1^N|I|}$, $h(\theta)$ has the form $0.\psi_1\psi_2\ldots\psi_N\theta_{N+1}\theta_{N+2}$ where $\theta_i \in \{0,1\}$. This in turn implies that $d(h(\psi), h(\theta)) < \epsilon$. Thus h is continuous. ■

Now, we can state a theorem regarding the dynamics of $f_{\eta,\nu}$ on Λ that is precisely the same as theorem 1, which describes the dynamics of σ on Σ. The sequence of points generated by repeated application of the map $f_{\eta,\nu}$ to a point in Λ is called an *orbit* of $f_{\eta,\nu}$. An orbit of $f_{\eta,\nu}$ is *i-periodic* (or has *period i*) if i is the least positive integer such that $f^i_{\eta,\nu}(x) = x$ for all x in the orbit. We say that an orbit $\mathcal{O}$ is *eventually i periodic* if there exists a finite number M in $\mathbb{N}$ such that the sequence in Λ obtained by calculating $\{f^M_{\eta,\nu}(x)\}$ for every $x \in \mathcal{O}$ forms an i periodic orbit. Any orbit that is neither periodic nor eventually periodic is said to be *nonperiodic*.

Theorem 3 *The map $f_{\eta,\nu}$ has*
1. countably many periodic orbits of arbitrarily high periods;
2. uncountably many nonperiodic orbits;
3. a dense orbit.

Proof: First, we show that $f_{\eta,\nu}$ acting on Λ and σ acting on Σ are topological conjugates, i.e. $h \circ f_{\eta,\nu}(\phi) = \sigma \circ h(\phi)$ for all $\phi \in \Lambda$. Let $\phi \in \Lambda$. Therefore, there exists a binary sequence, $\{\alpha_k\}$ such that $\phi = \bigcap_{n=1}^{\infty} I_{\alpha_1\alpha_2\ldots\alpha_n}$. Therefore $f_{\eta,\nu}(\phi) = \bigcap_{n=2}^{\infty} I_{\alpha_2\alpha_3\ldots\alpha_n}$. From the definition of σ, we have $h(f_{\eta,\nu}(\phi)) = .\alpha_2\alpha_3\ldots$ and $\sigma(h(\phi)) = \sigma(.\alpha_1\alpha_2\ldots) = (.\alpha_2\alpha_3\ldots)$. This shows that $h \circ f_{\eta,\nu}(\phi) = \sigma \circ h(\phi)$.

The theorem is an immediate consequence of topological conjugacy of f acting on Λ with σ acting on Σ and theorems 1 and 2. ■

3 Noninelastic Impacts ($\epsilon \neq 0$)

In this section we shall study the impacts that have very small coefficient of restitution, and in particular we will study the case with $\epsilon = 0.01$. These impacts are essentially different from the inelastic impacts as they are characterized by the knowledge of the 'position' and 'velocity' variables while inelastic impacts are determined solely by the 'position' variable. Mathematically, inelastic impacts are described by one dimensional systems while the noninelastic impacts are determined by two dimensional systems. We have already seen in section (1) that under the condition $x(t) - z(t) > 0$ for all $t \in (t_k, t_{k+1})$, the two dimensional system describing the impact at time instant t_{k+1} is given by equations (8) and (9). Using the dimensionless variables introduced in section (1) and the nondimensionalised velocity variable $\gamma_k := \frac{v_k}{\omega_n p}$, we can rewrite these equations as

$$\begin{aligned}(1 + \nu\sin(\psi_k))\cos(\eta\psi_{k+1} - \eta\psi_k) \qquad (11)\\ +(\epsilon\gamma_k + \frac{\nu}{\eta}(1+\epsilon)\cos(\psi_k))\sin(\eta\psi_{k+1} - \eta\psi_k)\\ -1 - \nu\sin(\psi_{k+1}) = 0,\end{aligned}$$

$$\begin{aligned}\gamma_{k+1} = (1 + \nu\sin(\psi_k))\sin(\eta\psi_{k+1} - \eta\psi_k) \qquad (12)\\ -(\epsilon\gamma_k + \frac{\nu}{\eta}(1+\epsilon)\cos(\psi_k))\cos(\eta\psi_{k+1} - \eta\psi_k).\end{aligned}$$

We see that, given the characteristics of impact at instant t_k, the impact phase $\phi_k := \psi_k$ modulo 2π and the dimensionless velocity γ_k; we can determine the characteristics $(\phi_{k+1}, \gamma_{k+1})$ of the next impact. We denote this map that takes the phase, ϕ, and velocity, γ, from one impact to the next by

$$F_{\eta,\nu,\epsilon} : (\phi, \gamma) \to (\phi, \gamma).$$

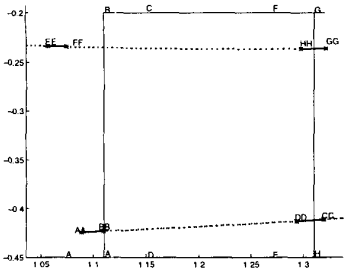

Figure 3: The topological horseshoe

We will show the existence of a two dimensional complex invariant set Λ_2 analogous to Λ in the one dimensional case, for a specific set of values, $(\eta, \nu, \epsilon) = (0.2121, -0.2, 0.01)$. We consider the images of the rectangle $ABCD$ and $EFGH$ under the map $F_{\eta,\nu,\epsilon}$ (see Figure (3)),where

$$ABCD = \{(\phi, \gamma) : 1.11 < \phi < 1.15, -0.45 < \gamma < 0\},$$
$$EFGH = \{(\phi, \gamma) : 1.27 < \phi < 1.32, -0.45 < \gamma < 0\}.$$

These images are shown in the same figure with emphasized points (e.g. AA) being the image of points (e.g. A). Note that the vertical distances are greatly contracted and the horizontal distances are expanded. We denote the vertical strips by $V_1 = ABCD$ and $V_2 = EFGH$ and their respective images (horizontal strips) by H_1 and H_2. We see that

$$F_{\eta,\nu,\epsilon}(V_i) = H_i, i = 1, 2$$

and thus we have a *topological horseshoe* [6]. For more detailed references on horseshoes, see [5] and [2]. Let $D = V_1 \cup V_2$. We define the invariant set Λ_2 by

$$\Lambda_2 = \bigcap_{n=-\infty}^{n=\infty} F_{\eta,\nu,\epsilon}(D).$$

$F_{\eta,\nu,\epsilon}$ having a horseshoe implies that Λ_2 contains [5],[2],[6]

1. countably many periodic orbits of arbitrarily high periods;
2. uncountably many nonperiodic orbits;
3. a dense orbit.

4 Analysis of the Mappings $f_{\eta,\nu}$ and $F_{\eta,\nu,\epsilon}$.

In previous sections, we have shown that for a specific set of parameters, $(\eta, \nu, \epsilon) = (.2121, -0.2, 0.0)$, the motion of the mass is complex on the invariant set $\Lambda \subset [1.11, 1.32]$ (in the inelastic-impact case). We have seen that the trajectories of the mass are sensitive to initial conditions on this set. It is also possible to show that this set has zero lebesgue measure. This means that there is a zero probability of 'typical' trajectories being in this set. In this section we shall investigate how this system behaves outside this set.

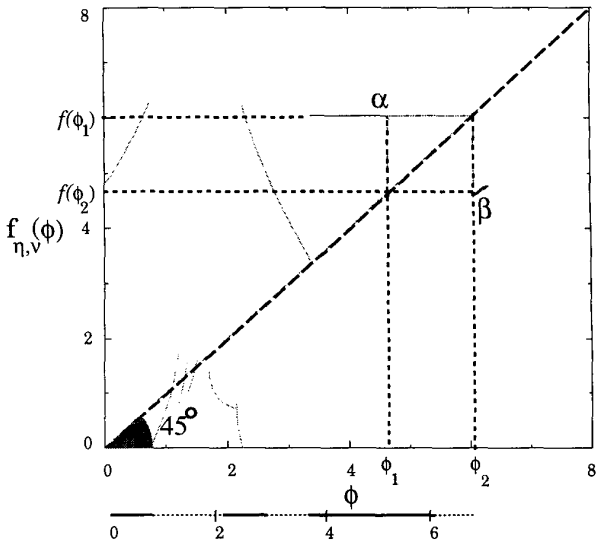

Figure 4: The graph of $f_{\eta,\nu}(\phi)$ for $\phi \in [0, 2\pi]$ is shown by the faint (curved) lines. $(\phi_1, \phi_2) = (4.64, 6.05)$ are on 2- periodic orbit. Simulation was done for $\phi \in [0, 2\pi]$ and $(\eta, \nu) = (.2121, -0.2)$. $f_{\eta,\nu}(\phi) = \phi$ on the dashed line.

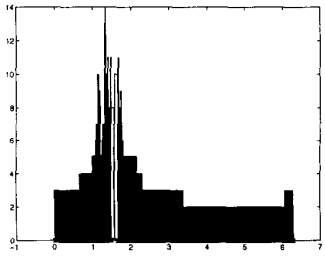

Figure 5: The Histogram showing the number of impacts before reaching stable 2- periodic orbit of $f_{\eta,\nu}(\phi)$. Simulation was done for $\phi \in [0, 2\pi], (\eta, \nu, \epsilon) = (.2121, -0.2, 0.0)$.

In Figure 4, we show the graph of $f_{\eta,\nu}$ over its full domain, i.e. $[0, 2\pi)$. We see that $\frac{\partial f_{\eta,\nu}}{\partial \phi}(\phi) = 0$ for all $\phi \in (3.38, 6.04)$. Impacts at these values are followed by a time interval in which the mass sticks on to the table. This happens when the force exerted on the mass by the spring is less than the force exerted on it by the table. This leads to a 2-periodic orbit (Note that, $\phi_2 = f_{\eta,\nu}(\phi_1)$ and $\phi_1 = f_{\eta,\nu}(\phi_2)$, and therefore, $\phi_i = f^2_{\eta,\nu}(\phi_i), i \in \{1, 2\}$ implying a 2-periodic orbit). We also see that all the orbits (that were simulated) eventually converge to this orbit. That is, this 2-periodic orbit attracts all the initial conditions chosen. The thickened part of the ϕ-axis shown in Figure 4 is a subset of the set of initial conditions that are

attracted to the stable orbit. Note that, the proof of $f_{\eta,\nu}$ being sensitive to the initial conditions in the set $[1.11, 1.32]$ depended only on the geometrical attributes of the graph of $f_{\eta,\nu}$ (i.e. the slope and the non invertibility), and we see the graph has the same properties in the set $[1.32, 1.48]$. This suggests the existence of another invariant set. So, although most of the initial conditions are attracted to the stable 2-periodic orbit, existence of these invariant sets shows that the dynamics of the mass in this model is complex. In Figure 5, we have plotted histograms with the height of the bar denoting the number of impacts before which the trajectory reaches the periodic orbit. We observe that there is a relatively large transience (before settling to periodic orbits) corresponding to initial conditions near the invariant sets. This shows the effect of the invariant sets on the dynamics of the system.

Similar simulations were done in the non-inelastic case for the same values of η and ν as in the one dimensional (inelastic impact) case with different values of the coefficient of restitution ϵ. In these cases too, we observed that, there is a stable 2-periodic orbit which attracts all the initial conditions chosen. We saw that the trajectories took longer time to reach the periodic orbit with increase in values of coefficient of restitution. This fact can be utilized in order to predict the coefficient of restitution between the plate and the mass.

5 Single Impact Periodic Orbits

In previous section we have analyzed the dynamics of the mass in the spring-mass system with specified values of the amplitude ν and frequency ratio η. In this section we will study the dynamics of $f_{\eta,\nu}$ in the whole parameter space. We had mentioned earlier that it is difficult to get the evolution of impact phases as the equation (eq.(10)) describing it is transcendental. However, we can analyze this equation for single-impact-periodic orbits. These orbits are said to occur if every impact occurs at the same phase (i.e. position) of the plate with the same velocity of the mass at every impact. In the inelastic case, the motion of the mass after an impact is completely determined by the phase value at the impact, and hence impacts occurring with the same phase ensure single impact periodic orbits. An n-periodic single impact orbit is one in which the two consecutive nondimensionalized impact times (see section (2)) differ by $2\pi n$. Substituting this condition in equation (10), we can show that the fixed point ϕ of the map is given by

$$(1+\nu\sin(\phi))\cos(2\pi n\eta) + \frac{\nu}{\eta}\cos(\phi)\sin(2\pi n\eta) - 1-\nu\sin(\phi) = 0. \quad (13)$$

We define $\alpha := \eta(1-\cos(2\pi n\eta)), \beta := \sin(2\pi n\eta)$ and $\theta := tan^{-1}(\frac{\beta}{\alpha})$. It can be seen that the equation (13) can be rewritten as

$$\sin(\phi-\theta) + \frac{\cos(\theta)}{\nu} = 0; \quad (14)$$

which gives explicit solution for ϕ. Note that all these calculations are valid under the assumption that the mass and the table separate just after the impacts and that 'sticking' does not occur. Now the stability of these fixed points can be determined by checking if the magnitude of the slope, $\frac{\partial f_{\eta,\nu}}{\partial\phi}(\phi)$, is less than unity. The slope is given by

$$\frac{\partial f_{\eta,\nu}}{\partial\phi}(\phi) = \frac{\frac{\gamma}{\eta}\sin(\phi)\sin(2\pi n\eta) + \eta(1-\gamma\sin(\phi))\sin(2\pi n\eta)}{\eta(1-\gamma\sin(\phi))\sin(2\pi n\eta) + \gamma\cos(\phi)\cos(2\pi n\eta) - \gamma\cos(\phi)}. \quad (15)$$

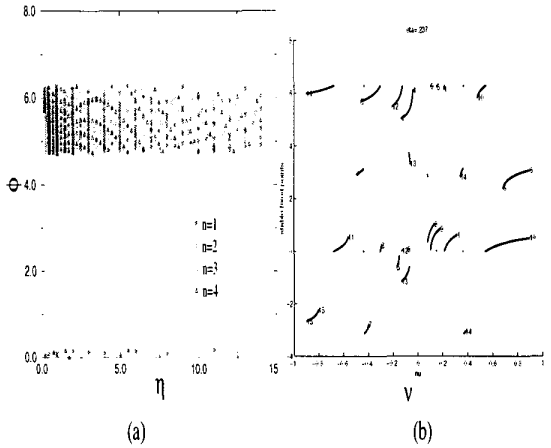

Figure 6: (a)The n-periodic fixed points with change in η with $\nu = 0.2$. (b) The n-periodic fixed points with change in ν with $\eta = 0.237$. The numbers on top of the curves denote the value of n.

The Figure 6(a) shows the various stable n-periodic fixed points as we vary η over the values $(0.01, 14)$. We see that slight changes in η lead to fixed points of periodic orbits of different periods. This shows that in this range of values of η, the motion of the mass is sensitve to the values of the frequency ratio, η.

The Figure 6(b) shows how the n-periodic fixed points vary as we change ν over the values $(-0.9, 0.9)$ for a fixed $\eta = 0.237$. Again we observe that slight changes in ν leads to fixed points of different periodic orbits. This implies that the motion of mass is sensitive to changes in the amplitude ratio (ν) of the system. Note that, in a n-periodic orbit, the table oscillates n times between consecutive impacts. Thus the impact frequency is a subharmonic of the frequency of the table. In the following section, we show experimental evidence of appearance of subharmonics on varying the amplitude of vibration of the table.

6 Experimental Study

In previous sections, we showed the presence of complicated dynamics exhibited by the model we developed. In this section we will present experimental results which show the sensitivity of periodic orbits to the amplitude of vibration. The experimental setup is shown in Figure 7. The cantilever has a length of $45\mu m$, thickness of $2\mu m$ (approx.) and width of $47\mu m$. Its tip's displacement is measured by reflecting laser beam off the back of the cantilever into an array of photodiodes. An adequate model of the cantilever dynamics is

$$\ddot{y} + 2\xi\omega_o\dot{y} + \omega_o^2 y = f(t),$$

where ξ is the damping factor, ω_o is the natural frequency and $f(t)$ is the external force applied to the cantilever. The damping factor is due to surrounding air which can be neglected. Thus the cantilever motion is described by

$$\ddot{y} + \omega_o^2 y = f(t).$$

For the experiment, a steel puck was glued to the top of a piezo disc of thickness $1mm$ (approx.) and diameter $10mm$. Mica wafer was attached to the steel puck. An insulator was glued to the bottom of the piezo disc which was firmly held to the base via another steel puck. Electrical leads were soldered to the top and bottom of the piezo which were connected to a signal source.

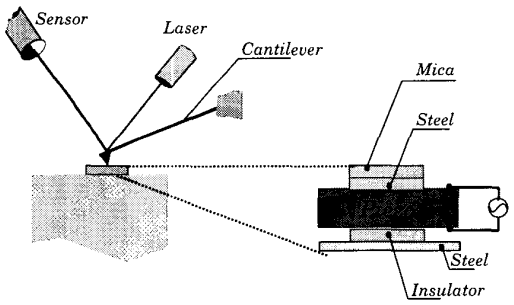

Figure 7: The Experimental Setup.

A sinusoidal voltage was applied to the piezo-disc at a frequency of $50kHz$. Figure 8 shows the effect of increasing the amplitude of vibration on the displacement of the cantilever. As can be seen there is eighth subharmonic appearing as the amplitude is increased, as predicted by the theory. This is indicative of chaos as predicted by the model. Further experiments to observe chaotic behavior are being conducted.

7 Conclusion

We have studied the dynamics of the mass in the mass-spring-vibrating table model (with inelastic impacts) for a particular set of parameter values and have proved that there exist countably many periodic orbits, uncountably many nonperiodic orbits and a dense orbit in the invariant set, Λ. We considered the case in which impacts are not inelastic (but with small coefficient of restitution) and showed the existence of another complex invariant set Λ_2 which implied complicated dynamics analogous to the one dimensional (inelastic) case. We also showed existence of a stable 2-periodic orbit which attracted most of the initial conditions. This 2-periodic orbit persisted in the two dimensional (non-inelastic) case. We found that these dynamics were sensitive to changes in the values of the frequency ratio, η, and the amplitude ratio, ν. An experimental study corroborated the complexity of the dynamics described.

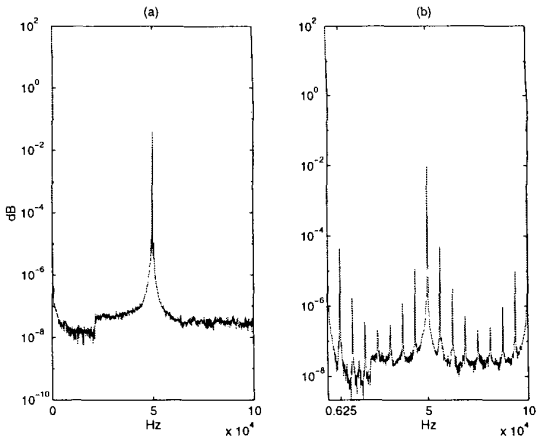

Figure 8: The sample is vibrated at the resonant frequency of the cantilever. The vertical axis reflects the displacement of the cantilever tip. In (a) the amplitude of vibration is lower and in (*b*) it is increased.

References

[1] M. B. Hindmarsh and D. J. Jefferies, "On the motions of the offset impact oscillator" *J Phys A:Math. Gen.* , 17,1994,pp.1791–1803.

[2] J. Guckenheimer and P. Holmes, "Nonlinear Oscillations,Dynamical Systems And Bifurcation Of Vector Fields", *Springer Verlag,Applied Mathematical Sciences* 42,pp.104-16.

[3] A.M. Bruckner,J.B. Bruckner and B.S. Thomson, "Real Analysis", Prentice Hall, New Jersey,pp. 271-75.

[4] Walter Rudin, "Principles of Mathematical Analysis" McGraw-Hill Inc, pp.30-31.

[5] S. Wiggins, "Introduction to Applied Nonlinear Dynamical Systems and Chaos", Springer Verlag,Texts In Applied Mathematics.

[6] J. Moser, "Stable and Random Motions in Dynamical Systems", Princeton University Press.